Chinese Journal of
POLYMER SCIENCE

RESEARCH ARTICLE

https://doi.org/10.1007/s10118-024-3080-1
Chinese J. Polym. Sci. **2024**, *42*, 1321–1332

Self-assembly Induced by Complexation of Diblock Copolyelectrolytes and Oppositely Charged Homopolymers

Ling Zhao[a], Zhi-Yuan Yin[b], Jia-Di Jiang[a], Er-Qiang Chen[a*], and Shuang Yang[a*]

[a] *Beijing National Laboratory for Molecular Sciences, Key Laboratory of Polymer Chemistry and Physics of Ministry of Education, Center for Soft Mater Science and Engineering, College of Chemistry and Molecular Engineering, Peking University, Beijing 100871, China*
[b] *Beijing National Laboratory for Molecular Sciences, College of Chemistry and Molecular Engineering, Peking University, Beijing 100871, China*

Abstract We investigate the solution self-assembly of a mixture of positively charged homopolymers and AB diblock copolymers, in which the A blocks are negatively charged, and the B blocks are neutral. The electrostatic complexation between oppositely charged polymers drives the formation of many ordered phases. The microstructures and phase diagrams are calculated using self-consistent field theory (SCFT) based on an ion-pair model with an equilibrium constant K to characterize the strength of binding between positively and negatively charged monomers. The effects of the charge ratio, representing the ratio of charges from the homopolymer over all charges from polymers in the system, on the ordered structure are systematically studied, both for hydrophobic and hydrophilic A blocks. The charge ratio plays an important role in determining the phase boundaries in the phase diagram of salt concentration versus polymer concentration. We also provide information about the varying tendency of the domain spacing and core size of the spherical phase when the charge ratio is changed, and the results are in good agreement with experiments. These studies provide a deep understanding of the self-assembled microstructures of oppositely charged diblock copolymer-homopolymer systems.

Keywords Self-assembly; Polyelectrolyte complexation; Self-consistent field theory; Ion-pair

Citation: Zhao, L.; Yin, Z. Y.; Jiang, J. D.; Chen, E. Q.; Yang, S. Self-assembly induced by complexation of diblock copolyelectrolytes and oppositely charged homopolymers. *Chinese J. Polym. Sci.* **2024**, *42*, 1321–1332.

INTRODUCTION

The self-assembly of AB diblock copolymer systems provides an important strategy for designing new functional materials due to the resulting variety of ordered nanostructures. A simple way to obtain these nanostructures is by adding homopolymers, thus avoiding the complex synthesis of new chemical compounds. In recent years, many studies have focused on neutral diblock copolymer-homopolymer systems that are partitioned by block incompatibility[1–13] or bound by hydrogen bonds.[14–20] Another interesting method involves introducing opposite charges on the same block (such as the A block) of different chains while keeping the B block neutral. This results in half of the copolymers having positively charged A blocks, and the other half carrying negative charges. In solution, these oppositely charged block copolymers undergo complex coacervation to generate various microphase-separated structures, such as ordered nanostructures and micelles.[21–26] The formed materials, also referred to as "electrostatic hydrogel", are widely used in batteries,[27–29] drug delivery,[30–32] and other fields. Compared with neutral block copolymer systems, the introduction of charges increases the diversity of property modulation and introduces more complex factors,[33] such as temperature,[34,35] pH,[35] solvent quality,[36,37] salt concentration,[38,39] *etc.*

A prominent feature of the above electrostatic hydrogel is that the micro-phase separated morphologies may be induced purely by strong electrostatic force, even if the neutral A/B blocks are miscible. The theoretical description of the self-assembly of this hydrogel is still limited. Fridrickson *et al.* developed an "embeded fluctuation model" to simulate the electrostatic attraction between two oppositely charged blocks.[40] Later, Sing *et al.* studied the formed morphologies by using chain adsorption model and transfer matrix theory.[41] However, these theories could provide only qualitative rather than quantitative predictions for the structures and phase diagrams. Our group[42,43] has developed a self-consistent field theory for electrostatically driven diblock polyelectrolyte coacervation using the ion-pair model in recent years, and our theory is in good agreement with the experiments.

Blending charged homopolymers with oppositely charged block copolymers provides a convenient and efficient way to design self-assembled materials.[44–54] The early studies focused on the dilute solution of polyelectrolyte-neutral diblock copolymers and linear chains with opposite charges, in which case the micelles were formed with charged components complex forming the core. The theory of micelle forma-

* Corresponding authors, E-mail: eqchen@pku.edu.cn (E.Q.C.)
E-mail: shuangyang@pku.edu.cn (S.Y.)

Special Issue: Charged Polymers
Received October 31, 2023; Accepted December 11, 2023; Published online January 26, 2024

tion in dilute solution mixtures was developed by Kramarenko *et al*.[36,55] The core of a micelle is formed by hydrophobic monomer units of polyelectrolyte complexes with opposite charges, while hydrophilic uncharged blocks of block copolymers form the micellar corona. They concluded that the formation of polyelectrolyte complexes and micelles is an association-decomposition reaction at specific chemical constants in solution, and calculated concentration distributions showed that micelles are formed from almost completely neutralized block copolymers, resulting in a micelle charge close to zero. This result corresponds well to the experimental results. Later, people paid more attention to concentrated solutions, where the long-range ordered microstructures may appear, due to their great potential application in developing hydrogel materials. Lemmers *et al*.[35,56] investigated electrostatic hydrogels formed by microphase separation of oppositely charged triblock copolymers and homopolymers that are reversible and multi-responsive. They found that salt concentration, polymer concentration and pH affect the size of micelles and the number of aggregates. However, the theoretical works about the ordered phases are rather limited. Bodrova *et al*.[57] calculated the microphase separation of oppositely charged diblock copolymers and homopolymers by means of strong segregation approximation, and suggested that the microphase separation originates from the relative stretching between the blocks. The phase diagrams were predicted for different combinations of parameters by adjusting the second virial coefficient, the fraction of charged blocks and the charge density of monomers.

Most studies handle the system with charge stoichiometry, *i.e*., the charges carried by polyanions are compensated by those from polycations completely. In reality, the charge composition is naturally a new variable since two charged moieties can be easily mixed in different ratios.[58] It has been recognized that the association of the oppositely charged moieties is strongest at stoichiometry point with a 1:1 charge ratio, which is a generic feature of charge-driven association.[59–61] However, there is a lack of clear understanding about what happens to the microstructures of polyelectrolyte complexes deviating from the charge stoichiometric point. In general, the excess charged polyanions will accumulate in the complexes, a similar phenomenon to the non-stoichiometric complexes of two oppositely charged homopolymers, and may progressively destabilize the self-assembly progress. Lemmers *et al*. presented a study on the influence of charge ratio on transient networks of polyelectrolyte complex micelles involving triblock copolymers for the first time,[62] and their results indicated that charge composition plays a crucial role in charge-driven association.

In this work, we extend our previous ion-pair model based SCFT to the self-assembled ordered structures of a charged homopolymer and oppositely charged-neutral diblock copolymers. Physically, our method is similar to the interpolymer-complexation model developed by Dehghan and Shi,[20] which was used to investigate the self-assembly of neutral diblock-homopolymer melt systems bound by hydrogen bonding. Our method deals with the electrostatic interactions explicitly. The ion-pair model assumes that the binding of positive and negative charges is reversible, that their binding has corresponding equilibrium constants, and that polymer-polymer binding is competitive with polymer-counterion binding. Next, we predict the spatial distribution of ion-pairs, monomers, and the electrostatic potential under different conditions. Additionally, we analyze the effect of charge composition on the structures, as well as the associated phase diagrams, in detail.

THEORETICAL MODEL

The entire system is assumed to be in contact with a heat bath with a constant temperature and ionic concentration, making it a typical semi-grand canonical ensemble. The system with a volume of V includes n_{p1} homopolymer chains and n_{p2} diblock copolymer chains. Each polyelectrolyte homopolymer is modeled as a continuous Gaussian chain consisting of A_1 monomers, and the diblock copolymer is modeled as a continuous Gaussian chain consisting of two monomers, A_2 and B_2. The A_1 monomer is positively charged, and its ionized counterion is denoted by C_1. In contrast, for the A_2B_2 chain, the A_2 monomer is negatively charged while the B_2 monomer is neutral, and the counterion of A_2 monomer is denoted by C_2, see Fig. 1. For simplicity, we assume that the salt ions added to the system consist of counterions C_1 and C_2. Water molecules are denoted by S.

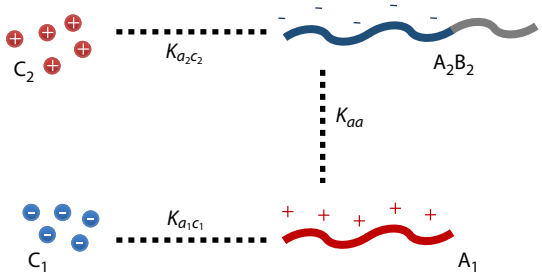

Fig. 1 Theoretical model.

The degree of polymerization of the diblock copolymer is N_2, and the numbers of monomers in the two blocks, A_2 and B_2, are expressed as N_{A_2} and N_{B_2}, respectively. We have $N_{A_2} + N_{B_2} = N_2$. The degree of polymerization of the homopolymer is N_1. The number of salts is denoted by n_{salt}, while the number of water molecules is denoted by n_S. z_{A_1} and z_{A_2} are used to represent the charges carried by each monomer, and z_{C_1} and z_{C_2} represent the charge valency of different counterions, with n_{C_1} and n_{C_2} denoting the total number of counterions C_1 and C_2, respectively. The Kuhn length of different blocks is set as $b_A = b_B = b$. The volumes of each type of monomer, counterion, and water are denoted as v_{A_1}, v_{A_2}, v_B, v_{C_1}, v_{C_2}, and v_S. For simplicity, we set $v_{A_1} = v_{A_2} = v_A$. The volume fraction of the charged block is denoted as f_{A_2}, and it is given by $f_{A_2} = N_{A_2}v_A/(N_{A_2}v_A + N_{B_2}v_B)$.

The microscopic concentrations of different components, A_1, A_2, B_2, C_1, C_2 and S in spatial position $\mathbf{r}$, are defined by

$$\hat{\rho}_\alpha(\mathbf{r}) = \sum_{i=1}^{n_p} \int_0^{N_\alpha} \mathrm{d}s\delta(\mathbf{r} - \mathbf{R}_i^\alpha(s)) \quad (1)$$

$$\hat{\rho}_\beta(\mathbf{r}) = \sum_{i=1}^{n_\beta} \delta(\mathbf{r} - \mathbf{r}_i^\beta) \quad (2)$$

In this study, the character α represents monomer species A_1, A_2, B_2, and β represents small molecules C_1, C_2, and S. $\mathbf{R}_i^\alpha(s)$ denotes the position of the s^{th} monomer along the α-block of the i^{th} polymer chain. $\mathbf{r}_i^\beta$ denotes the position of the

i^{th} small molecule β.

The complexation between charged components is modeled by the formation of ion-pairs between oppositely charged monomers or monomer/counterion. In the dynamic association process between positive charge and negative charge, we account for the ion-pairs by considering the following reversible dynamic equilibrium:

$$A_1^+ + C_1^- \rightleftharpoons [A_1C_1]$$
$$A_2^- + C_2^+ \rightleftharpoons [A_2C_2]$$
$$A_1^+ + A_2^- \rightleftharpoons [A_1\ A_2]$$

where, $[A_1C_1]$, $[A_2C_2]$ and $[A_1A_2]$ represent the different associated ion-pairs with corresponding equilibrium constants $K_{a_1c_1}$, $K_{a_2c_2}$ and $K_{a_1a_2}$. There are three different reaction sites on a charged A_1 chain, as shown in Fig. 1, including purely charged sites (denoted by a_1), neutralized sites being paired with C_1 (denoted by a_1c_1), and neutralized sites being paired with monomers A_2 from the charged A_2 block (denoted by a_1a_2). The A_2 chain has similar three sites denoted by a_2, a_2c_2, and a_1a_2, respectively. Consequently, five reaction sites on the A block exist in our system, and we use n_{a_1}, n_{a_2}, $n_{a_1c_1}$, $n_{a_2c_2}$, $n_{a_1a_2}$ to represent their quantities. Finally, the fractions of each type of site, which give the ratio of the number of this site to the total number of monomer (A_1 or A_2) locally, are defined as

$$\hat{f}_1(\mathbf{r}) = \sum_{i=1}^{n_{a_1}} \delta(\mathbf{r} - \mathbf{r}_i^{a_1})/\hat{\rho}_{A_1}(\mathbf{r}) \tag{3}$$

$$\hat{f}_2(\mathbf{r}) = \sum_{i=1}^{n_{a_2}} \delta(\mathbf{r} - \mathbf{r}_i^{a_2})/\hat{\rho}_{A_2}(\mathbf{r}) \tag{4}$$

$$\hat{g}_1(\mathbf{r}) = \sum_{i=1}^{n_{a_1c_1}} \delta(\mathbf{r} - \mathbf{r}_i^{a_1c_1})/\hat{\rho}_{A_1}(\mathbf{r}) \tag{5}$$

$$\hat{g}_2(\mathbf{r}) = \sum_{i=1}^{n_{a_2c_2}} \delta(\mathbf{r} - \mathbf{r}_i^{a_2c_2})/\hat{\rho}_{A_2}(\mathbf{r}) \tag{6}$$

$$\hat{h}_1(\mathbf{r}) = \sum_{i=1}^{n_{a_1a_2}} \delta(\mathbf{r} - \mathbf{r}_i^{a_1a_2})/\hat{\rho}_{A_1}(\mathbf{r}) \tag{7}$$

$$\hat{h}_2(\mathbf{r}) = \sum_{i=1}^{n_{a_1a_2}} \delta(\mathbf{r} - \mathbf{r}_i^{a_1a_2})/\hat{\rho}_{A_2}(\mathbf{r}) \tag{8}$$

In terms of their physical meaning, f_1, g_1, h_1 represent the fractions of different reaction sites on the charged A_1 chain. These fractions must satisfy $\hat{f}_1(\mathbf{r}) + \hat{g}_1(\mathbf{r}) + \hat{h}_1(\mathbf{r}) = 1$ for the charged A_1 block as well as $\hat{f}_2(\mathbf{r}) + \hat{g}_2(\mathbf{r}) + \hat{h}_2(\mathbf{r}) = 1$ for the charged A_2 block.

In order to emphasize the role of mobile ions, we adopt the semi-grand canonical ensemble to handle the system. The number of copolymer chains is fixed, while the chemical potentials of other small molecules (small ions and solvents) are determined by the reservoir. The Hamiltonian of our system includes four contributions: $H = H_{\text{ela}} + H_{\text{int}} + H_{\text{ele}} + H_{\text{chem}}$. The first term, H_{ela}, represents the elastic energy due to the stretching of polymer chains. The second term, H_{int}, denotes the incompatible interaction energy between different components, and we ignore the excluded volume interactions related to counterions. The third term, H_{ele}, accounts for the electrostatic interaction energy. The last term, H_{chem}, arises from the contributions derived from the chemical potentials of each species, indicating the binding energy of ion-pairs.

Given the Hamiltonian, the partition function can be expressed in terms of the functional integral over all degrees of freedom. After the standard processing of SCFT,[63] one can obtain the mean field free energy from the partition function. Further details can be found in our previous publication.[43] Regarding the dimensions, for simplicity we adopt the dimensionless mean field density of species j, denoted as $\rho_j(\mathbf{r})$ with respect to the reference density $\rho_0 = 1/b^3$. In the following expression, the mean field density $\rho(\mathbf{r})$ actually represents $\rho(\mathbf{r})/\rho_0$. We set the Kuhn length b as the length unit and choose $b = 1$ nm . The volumes of monomers and solvents are assumed to be the same and equal to the unit volume b^3, *i.e.*, $v_A = v_B = v_S = 1$. The volumes of small ions are considered negligible, *i.e.*, $v_{C1} = v_{C2} = 0$ for C_1 and C_2. The final mean field free energy is given by

$$\begin{aligned}\beta F = \int \mathrm{d}\mathbf{r}\Big[& -\sum\nolimits_j \omega_j(\mathbf{r})\rho_j(\mathbf{r}) \\ & + \chi_{AB}\rho_A(\mathbf{r})\rho_B(\mathbf{r}) + \chi_{SA}\rho_S(\mathbf{r})\rho_A(\mathbf{r}) \\ & + \chi_{SB}\rho_S(\mathbf{r})\rho_B(\mathbf{r}) \\ & + \beta e\psi(\mathbf{r})\rho_e(\mathbf{r}) - \frac{1}{2}\beta\varepsilon\,|\nabla\psi(\mathbf{r})|^2 \\ & - \big(\gamma_{f_1}(\mathbf{r})f_1(\mathbf{r}) + \gamma_{g_1}(\mathbf{r})g_1(\mathbf{r}) + \gamma_{h_1}(\mathbf{r})h_1(\mathbf{r})\big)\rho_{A_1}(\mathbf{r}) \\ & - \big(\gamma_{f_2}(\mathbf{r})f_2(\mathbf{r}) + \gamma_{g_2}(\mathbf{r})g_2(\mathbf{r}) + \gamma_{h_2}(\mathbf{r})h_2(\mathbf{r})\big)\rho_{A_2}(\mathbf{r}) \\ & + \eta(\mathbf{r})\Big(\sum\nolimits_j v_j\rho_j(\mathbf{r}) - 1\Big) \\ & + \alpha_1(\mathbf{r})\rho_{A_1}(\mathbf{r})\big(f_1(\mathbf{r}) + g_1(\mathbf{r}) + h_1(\mathbf{r}) - 1\big) \\ & + \alpha_2(\mathbf{r})\rho_{A_2}(\mathbf{r})\big(f_2(\mathbf{r}) + g_2(\mathbf{r}) + h_2(\mathbf{r}) - 1\big)\Big] \\ & - n_{p_1}\ln(VQ_{p_1}) + \ln(n_{p_1}!) - n_{p_2}\ln(VQ_{p_2}) + \ln(n_{p_2}!) \\ & - \sum\nolimits_m VQ_m\end{aligned} \tag{9}$$

where, β is equal to $1/k_BT$. The index j runs over all species in the system, including monomers (A_1, A_2, B_2), small ions (C_1, C_2), and solvent (S). $\rho_j(\mathbf{r})$ is the mean-field density of species j, and $\omega_j(\mathbf{r})$ is the conjugated external field for each species. The concentration of monomer A includes contributions from both A_1 and A_2. In the framework of mean field approximation, the electrostatic energy contribution (the fourth line in Eq. 9) comes from the inhomogeneous distribution of charge density ρ_e. If positively charged monomers are totally compensated by negatively charged monomers, the electrostatic potential should be zero everywhere due to a homogeneous charge density of $\rho_e(\mathbf{r}) = 0$. $\gamma_{f_1}(\mathbf{r})$, $\gamma_{f_2}(\mathbf{r})$, $\gamma_{g_1}(\mathbf{r})$, $\gamma_{g_2}(\mathbf{r})$, $\gamma_{h_1}(\mathbf{r})$, and $\gamma_{h_2}(\mathbf{r})$ are the conjugated fields corresponding to local fraction distributions of the sites $f_1(\mathbf{r})$, $f_2(\mathbf{r})$, $g_1(\mathbf{r})$, $g_2(\mathbf{r})$, $h_1(\mathbf{r})$, and $h_2(\mathbf{r})$. $\eta(\mathbf{r})$ is a Lagrangian multiplier to guarantee the incompressibility condition for each point. $\alpha_1(\mathbf{r})$ and $\alpha_2(\mathbf{r})$ are the Lagrangian multipliers to ensure the conservation conditions for f, g, and h. Q_{p_1} and Q_{p_2} are the partition functions of a single homopolymer chain A_1 and a single diblock copolymer A_2B_2, respectively. They are determined by the external fields and given by the following expressions:

$$Q_{p1} = \frac{1}{V}\int \mathrm{D}\{\mathbf{R}^1(s)\}\exp\{-H_{\text{cop}}^1\} \tag{10}$$

$$Q_{p2} = \frac{1}{V}\int \mathrm{D}\{\mathbf{R}^2(s)\}\exp\{-H_{\text{cop}}^2\}\delta\left(\mathbf{R}^{A_2}(N_{A_2}) - \mathbf{R}^{B_2}(N_{B_2})\right) \tag{11}$$

where H_{cop} is the Hamiltonian of a polymer chain in the external field, and it satisfies:

$$H_{\text{cop}}^1 = \int_0^{N_{A_1}} \mathrm{d}s\left[\frac{3}{2b^2}\left(\frac{\mathrm{d}\mathbf{R}^{A_1}(s)}{\mathrm{d}s}\right)^2 + \omega_{A_1}(\mathbf{R}^{A_1}(s))\right] \tag{12}$$

$$H^2_{\text{cop}} = \sum_{\alpha=A_2,B_2} \int_0^{N_\alpha} \mathrm{d}s \left[\frac{3}{2b^2} \left(\frac{\mathrm{d}\mathbf{R}^\alpha(s)}{\mathrm{d}s} \right)^2 + \omega_\alpha(\mathbf{R}^\alpha(s)) \right] \quad (13)$$

where Q_{m} is the partition functions for a single molecule of species m. Note that m includes all types of small molecules and different reaction sites on A chains. The specific expressions of Q_{m} can be found in the study.[43]

The set of SCF equations can be obtained by minimizing of βF with respect to each field and density in Eq. (9). The external fields are derived by setting the functional derivatives of βF with respect to $\rho_j(\mathbf{r})$ equal to zero, which follow as:

$$\omega_{A_1}(\mathbf{r}) = \chi_{AB}\rho_B(\mathbf{r}) + \chi_{SA}\rho_S(\mathbf{r}) - \alpha_1(\mathbf{r}) + \eta(\mathbf{r}) - 1 \quad (14)$$

$$\omega_{A_2}(\mathbf{r}) = \chi_{AB}\rho_B(\mathbf{r}) + \chi_{SA}\rho_S(\mathbf{r}) - \alpha_2(\mathbf{r}) + \eta(\mathbf{r}) - 1 \quad (15)$$

$$\omega_{B_2}(\mathbf{r}) = \chi_{AB}\rho_A(\mathbf{r}) + \chi_{SB}\rho_S(\mathbf{r}) + \eta(\mathbf{r}) \quad (16)$$

$$\omega_{C_1}(\mathbf{r}) = z_{C_1}\beta e\psi(\mathbf{r}) + \eta(\mathbf{r}) \quad (17)$$

$$\omega_{C_2}(\mathbf{r}) = z_{C_2}\beta e\psi(\mathbf{r}) + \eta(\mathbf{r}) \quad (18)$$

$$\omega_S(\mathbf{r}) = \chi_{SA}\rho_A(\mathbf{r}) + \chi_{SB}\rho_B(\mathbf{r}) + \eta(\mathbf{r}) \quad (19)$$

By setting the functional derivatives of βF with respect to $\omega_j(\mathbf{r})$ to zero, the densities $\rho_j(\mathbf{r})$ satisfy the equations as

$$\rho_{A_1}(\mathbf{r}) = \frac{n_{p_1}}{VQ_{p_1}} \int_0^{N_{A_1}} \mathrm{d}s q_{A_1}(\mathbf{r}, s) q_{A_1}(\mathbf{r}, N_{A_1} - s) \quad (20)$$

$$\rho_{A_2}(\mathbf{r}) = \frac{n_{p_2}}{VQ_{p_2}} \int_0^{N_{A_2}} \mathrm{d}s q_{A_2}(\mathbf{r}, s) q^+_{A_2}(\mathbf{r}, N_{A_2} - s) \quad (21)$$

$$\rho_{B_2}(\mathbf{r}) = \frac{n_{p_2}}{VQ_{p_2}} \int_0^{N_{B_2}} \mathrm{d}s q_{B_2}(\mathbf{r}, s) q^+_{B_2}(\mathbf{r}, N_{B_2} - s) \quad (22)$$

$$\rho_{C_1}(\mathbf{r}) = \exp(-\omega_{C_1}(\mathbf{r}) - \beta\mu_{C_1}) \quad (23)$$

$$\rho_{C_2}(\mathbf{r}) = \exp(-\omega_{C_2}(\mathbf{r}) - \beta\mu_{C_2}) \quad (24)$$

$$\rho_S(\mathbf{r}) = \exp(-\omega_S(\mathbf{r}) - \beta\mu_S) \quad (25)$$

where $q_{A_1}(\mathbf{r}, s)$ is the propagator of the A_1 chain, representing the probability of finding the end monomer of the A_1 block of length s at the point $\mathbf{r}$ with a free initial monomer. It satisfies the modified diffusion equations:

$$\frac{\partial q_{A_1}(\mathbf{r}, s)}{\partial s} = \frac{b^2}{6}\nabla^2 q_{A_1}(\mathbf{r}, s) - \omega_{A_1}(\mathbf{r}) q_{A_1}(\mathbf{r}, s) \quad (26)$$

with the initial conditions $q_{A_1}(\mathbf{r}, 0) = 1$.

The propagator $q_{A_2}(\mathbf{r}, s)$ has a similar physical meaning. However, since diblock copolymer is different from the homopolymer, we need another propagator $q^+_{A_2}(\mathbf{r}, s)$ that represents the probability of finding the end monomer of the A_1 chain of length s at $\mathbf{r}$, while the other part of A_1 chain is connected to the entire B_2 block.[42] $q_{A_1}(\mathbf{r}, s)$ and $q^+_{A_1}(\mathbf{r}, s)$ satisfy the equations as

$$\frac{\partial q_{A_2}(\mathbf{r}, s)}{\partial s} = \frac{b^2}{6}\nabla^2 q_{A_2}(\mathbf{r}, s) - \omega_{A_2}(\mathbf{r}) q_{A_2}(\mathbf{r}, s) \quad (27)$$

$$\frac{\partial q^+_{A_2}(\mathbf{r}, s)}{\partial s} = \frac{b^2}{6}\nabla^2 q^+_{A_2}(\mathbf{r}, s) - \omega_{A_2}(\mathbf{r}) q^+_{A_2}(\mathbf{r}, s) \quad (28)$$

with the initial conditions $q_{A_1}(\mathbf{r}, 0) = 1$ and $q^+_{A_2}(\mathbf{r}, 0) = q_{A_2}(\mathbf{r}, N_{A_2})$.

The other propagators for B block, $q_{B_2}(\mathbf{r}, s)$ and $q^+_{B_2}(\mathbf{r}, s)$, have similar definitions as those for A_2. Based on these quantities, Q_{p_1} and Q_{p_2} can then be evaluated by

$$Q_{p_1} = \frac{1}{V}\int \mathrm{d}\mathbf{r} q_{A_1}(\mathbf{r}, N_{A_1}) \quad (29)$$

$$Q_{p_2} = \frac{1}{V}\int \mathrm{d}\mathbf{r} q^+_{A_2}(\mathbf{r}, N_{A_2}) = \frac{1}{V}\int \mathrm{d}\mathbf{r} q^+_{B_2}(\mathbf{r}, N_{B_2}) \quad (30)$$

The remaining SCF equations can be obtained in the same way, and they follows:

$$f_1(\mathbf{r}) = \exp(-\gamma_{f_1}(\mathbf{r}) - \beta\mu_{a_1}), \quad f_2(\mathbf{r}) = \exp(-\gamma_{f_2}(\mathbf{r}) - \beta\mu_{a_2}) \quad (31)$$

$$g_1(\mathbf{r}) = \exp(-\gamma_{g_1}(\mathbf{r}) - \beta\mu_{a_1c_1}), \quad g_2(\mathbf{r}) = \exp(-\gamma_{g_2}(\mathbf{r}) - \beta\mu_{a_2c_2}) \quad (32)$$

$$h_1(\mathbf{r}) = \exp(-\gamma_{h_1}(\mathbf{r}) - \gamma_{h_2}(\mathbf{r}) - \beta\mu_{a_1a_2})\rho_{A_2}(\mathbf{r}) \quad (33)$$

$$h_2(\mathbf{r}) = \exp(-\gamma_{h_1}(\mathbf{r}) - \gamma_{h_2}(\mathbf{r}) - \beta\mu_{a_1a_2})\rho_{A_1}(\mathbf{r}) \quad (34)$$

$$\gamma_{f_1}(\mathbf{r}) = \alpha_1(\mathbf{r}) + z_{A_1}\beta e\psi(\mathbf{r}), \quad \gamma_{f_2}(\mathbf{r}) = \alpha_2(\mathbf{r}) + z_{A_2}\beta e\psi(\mathbf{r}) \quad (35)$$

$$\gamma_{g_1}(\mathbf{r}) = \alpha_1(\mathbf{r}) + \eta(\mathbf{r}), \quad \gamma_{g_2}(\mathbf{r}) = \alpha_2(\mathbf{r}) + \eta(\mathbf{r}) \quad (36)$$

$$\gamma_{h_1}(\mathbf{r}) = \alpha_1(\mathbf{r}), \quad \gamma_{h_2}(\mathbf{r}) = \alpha_2(\mathbf{r}) \quad (37)$$

$$f_1(\mathbf{r}) + g_1(\mathbf{r}) + h_1(\mathbf{r}) = 1, \quad f_2(\mathbf{r}) + g_2(\mathbf{r}) + h_2(\mathbf{r}) = 1 \quad (38)$$

$$\sum_j v_j\rho_j(\mathbf{r}) = 1 \quad (39)$$

$$\beta e\nabla^2\psi(\mathbf{r}) + 4\pi l_B\rho_e(\mathbf{r}) = 0 \quad (40)$$

Note that l_B in Eq. (40) is the Bjerrum length and is defined as $l_B = e^2/(\varepsilon k_B T)$.

Eqs. (14–40) constitute a closed set of SCF equations and need to be solved numerically. In Eqs. (23–25) and (9–34), the constant prefactors $\exp(-\beta\mu_{C_1})$, $\exp(-\beta\mu_{C_2})$, $\exp(-\beta\mu_S)$, $\exp(-\beta\mu_{a_1})$, $\exp(-\beta\mu_{a_2})$, $\exp(-\beta\mu_{a_1c_1})$, $\exp(-\beta\mu_{a_2c_2})$ and $\exp(-\beta\mu_{a_1a_2})$ are obtained from the bulk conditions $\rho^b_{C_1}$, $\rho^b_{C_2}$, ρ^b_S, f^b_1, f^b_2, g^b_1, g^b_2 and h^b, respectively. $\rho^b_{C_1}$ and $\rho^b_{C_2}$ are set to be equal to bulk salt concentration ρ_{salt} if the total charges of polymers are completely compensated. The three equilibrium constants are related to the parameters in the bulk solution *via*:

$$K_{a_1c_1} = \exp[-\beta(\mu_{a_1c_1} - \mu_{a_1} - \mu_{C_1})] = \frac{g^b_1}{f^b_1\rho^b_{C_1}} \quad (41)$$

$$K_{a_2c_2} = \exp[-\beta(\mu_{a_2c_2} - \mu_{a_2} - \mu_{C_2})] = \frac{g^b_2}{f^b_2\rho^b_{C_2}} \quad (42)$$

$$K_{aa} = \exp[-\beta(\mu_{a_1a_2} - \mu_{a_1} - \mu_{a_2})] = \frac{h^b}{f^b_1 f^b_2} \quad (43)$$

These constants measure the interaction strength of ion-pair formation. K_{aa} reflects the binding strength between oppositely charged monomers A_1 and A_2. $K_{a_1c_1}$ (or $K_{a_2c_2}$) reflects the binding strength between monomer A_1 (or A_2) and counterion C_1 (or C_2). For simplicity, we assume $K_{a_1c_1} = K_{a_2c_2} = K_{ac}$. K_{aa} and K_{ac} determine the strength of electrostatic correlations. Since all small ions are composed of the part binding with polymer chains and the part being dissociated from salts, we define the total concentration of small ions as $\rho^{\text{total}}_{C_1} = \rho_{C_1}(\mathbf{r}) + g_1(\mathbf{r})\rho_{A_1}(\mathbf{r})$ and $\rho^{\text{total}}_{C_2} = \rho_{C_2}(\mathbf{r}) + g_2(\mathbf{r})\rho_{A_2}(\mathbf{r})$.

With given systematic parameters, we solve the set of SCF equations using iteration methods to obtain densities and ex-

ternal fields for a specified ordered phase. Subsequently, the free energy density can be calculated. This article considers five ordered structures: lamellae phase (L), hexagonal phase (H_1) with A block comprising the cylinder core, inverse hexagonal phase (H_2) with a core of B block, body-centered cubic phase (B_1) with A block consisting of the core, and inverse cubic phase (B_2) with a core formed by the B block. For the complex phases (H and B), we use the unit-cell approximation to simplify the calculation.[43] The free energy density at equilibrium is determined by minimizing it with respect to the size of the unit cell. Subsequently, the phase diagram is constructed by comparing the free energy for different ordered structures. The morphology with the lowest energy density is chosen as the equilibrium phase for a set of given parameters.

RESULTS AND DISCUSSION

In order to emphasize the complexation effect of electrostatic interactions between oppositely charged chains, certain parameters are held constant in the calculations. We set b as the length unit. It is assumed that the charged A_2 block is structurally equivalent to the oppositely charged A_1 homopolymer chain, ensuring they have equal lengths, $N_1 = N_2 \cdot f_{A_2}$, and consequently, equal fractions of charged units. The polymerization degree of polymers is fixed at $N_2 = 100$. The charged monomers and small ions are monovalent, with $z_{A_1} = 1.0$, $z_{A_2} = -1.0$, $z_{C_1} = -1.0$, and $z_{C_2} = 1.0$. The Bjerrum length l_B is set to 0.7, which is a typical value for a water solution with $b = 1$ nm.

In our previous study on an oppositely charged diblock copolymer system,[43] the electrostatic potential of the system was nearly zero everywhere, attributed to the symmetry property of charge compensation from polyanions and polycations. In the present case, the homopolymer-diblock copolymer system can exhibit asymmetry, and the spatial variation of the electrostatic potential is not negligible. Therefore, we calculate the spatial distribution of the electrostatic potential, especially when the total charges carried by polymers are not fully compensated. The charge composition is defined following Lemmers *et al*.,[62] expressed as:

$$f_+ = \frac{[A_1]}{[A_1] + [A_2]} \tag{44}$$

where f_+ represents the ratio of the concentration of positively charged monomers from homopolymers to the concentration of all charged monomers, including both homopolymers and diblock copolymers, assuming the solution is homogeneous. The charge stoichiometry point corresponds to $f_+ = 0.5$. The entire system appears neutral because both the diblocks and the homopolymer have their own neutralizing counterions. Due to the charge mismatch between polymers when the charge composition of the system is not $f_+ = 0.5$, an overall salt concentration cannot be used to represent the concentrations of positive and negative free ions. In this study, we use the practical salt concentration ρ_{salt}^{add} to denote the salt concentration, where ρ_{salt}^{add} is the number of salt ions per unit volume of b^3. Taking C_1 as an example, the actual concentration of free C_1 in the system is ρ_{C_1}, given by $\rho_{C_1} = \left|\frac{\rho_{A_1} z_{A_1}}{z_{C_1}}\right| + \rho_{salt}^{add}$.

Before presenting the main results, we explore the effect of homopolymer length on the phase behavior. The calculations indicate that the phase regions and areas of the phase diagrams remain almost unchanged when the homopolymer length is varied (data not shown). Therefore, the homo-polyelectrolyte chains mainly play the role of "connecting" different A_2 blocks, and their length does not significantly affect the ordered structures. Similar self-assembly phenomena induced by charged homopolymers through electrostatic complexation have been observed by Duan *et al*.[37] In their study, the added cationic polyelectrolytes bind the dispersed ionomers and trigger their self-assembly into larger aggregates.

The Case of Hydrophobic Charged Chains

Since many factors affect the self-assembly process, we will consider both hydrophobic and hydrophilic charged blocks, while keeping the neutral blocks hydrophilic, as is common in experiment works.[56,62] Firstly, we explore the phase behavior of the system with hydrophobic charged blocks (including the charged homopolymers). The composition of the diblock copolymer is set as $f_{A_2} = 0.2$. With this choice, the complexation of charged components tends to constitute the core of ordered structures.

Fig. 2 displays the theoretical phase diagrams as a function of salt and polymer concentration for different charge compositions $f_+ = 0.3, 0.5, 0.7$. Several typical phases, including the homogeneous phase, B_1, H_1, and L, may appear. Due to the small ratio of charged blocks and hydrophobic charged blocks, no inverted phase structure is observed. As the polymer concentration decreases or the salt concentration increases, the ordered phases vary following the sequence L → H_1 → B_1 → Dis. This behavior is similar to the case of oppositely charged diblock copolymers.[39] At a low content of homopolymers with $f_+ = 0.3$, the L phase cannot be reached. With an increase in the charge composition, $f_+ = 0.5$ or 0.7, the phase boundaries shift to the left. At the same time, the regions of B_1 and H_1 become smaller, while that of the L phase becomes larger.

For a better understanding of the phase transition rule, we can analyze the results in terms of the volume fraction of charged components. By using the definition of f_+, one can derive that the concentration of positively charged monomers in a homogeneous solution is $[A_1] = [A_2] \times f_+/(1 - f_+)$. Then the total volume ratio of the complexation part from charged A blocks and homopolymers to the total polymers can be given by the formula:

$$v_{charge} = \frac{[A_1] + [A_2]}{[A_1] + [A_2] + [B_2]} = \frac{f_{A_2}}{f_{A_2} \cdot f_+ + 1 - f_+} \tag{45}$$

where $[B_2]$ denotes the monomer concentration of the B_2 block in the given homogeneous solution. We consider a special system with fixed parameters: $\phi_p = 0.5$ and $\rho_{salt}^{add} = 0$. Now, we add homopolymer content f_+ from 0.3 to 0.7, and v_{charge} varies from 0.263 to 0.455 accordingly. For a low content of homopolymers, the self-assembled structure is the B_1 phase. Adding more homopolymers leads to the phase transition from B_1 to H_1 to L, as shown in Fig. 2. If we regard the charged components (complexation part) as a whole, v_{charge} is similar to the composition of a neat diblock copolymer. Then, the phase transition sequence mentioned above is reasonable as a general

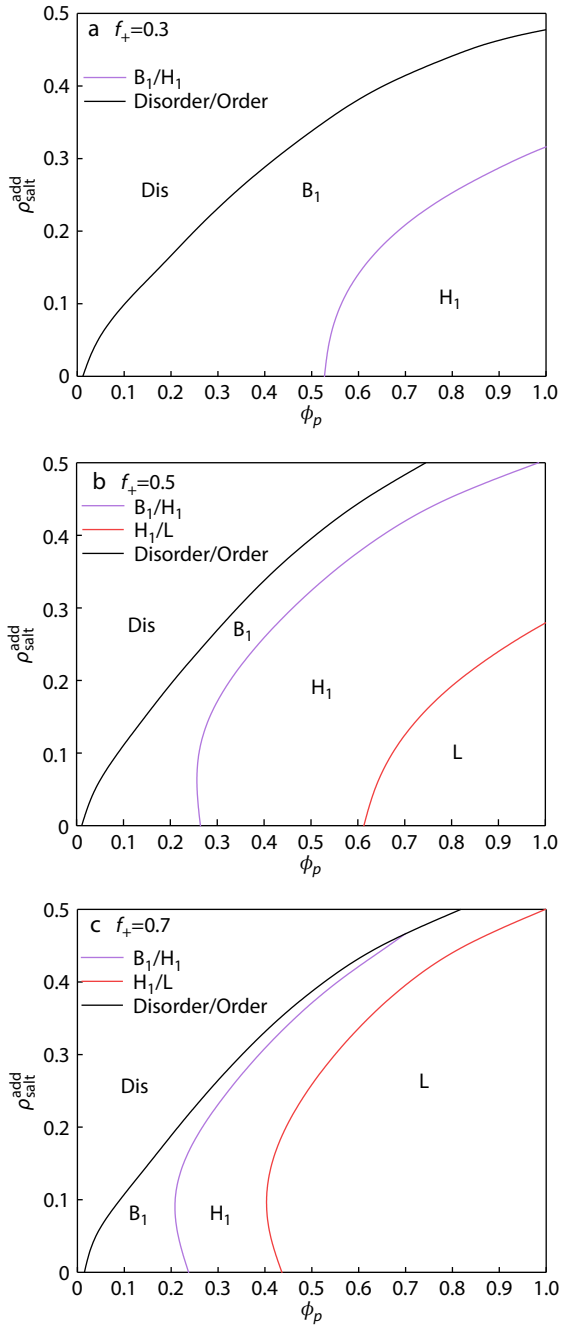

Fig. 2 Salt concentration (ρ_{salt}^{add}) versus polymer concentration (ϕ_p) phase diagram with different charge cases at $\chi_{AB}=0.05$, $\chi_{SA}=0.4$, $\chi_{SB}=0.0$, $N_1=20$, $N_2=100$, $f_{A_2}=0.2$, $K_{ac}=5$, $K_{aa}=10$. (a) $f_+=0.3$, (b) $f_+=0.5$, (c) $f_+=0.7$. Dis denotes disordered (homogeneous) phase, B_1 denotes the body-centered cubic phase with A blocks forming the cubic core, H_1 denotes the hexagonal cylinder phase with A blocks forming the cylinder core. L denotes the lamellae phase.

trend.

It is useful to analyze how the spatial distributions of monomer concentration and electrostatic potential are influenced by the added salt and charge composition. We only consider the B_1 phase under different conditions due to its close relationship with experiments. As the B_1 phase is spherically symmetric, we provide the concentration distribution and electrostatic potential distribution as functions of the separation from the sphere center. It is noted that in our calculation, the homogeneous system, in which the polymer and salt are uniformly distributed in space, is chosen as the reference state and has an electrostatic potential of zero.

Figs. 3(a), 3(c) and 3(e) display the profiles of A_1 monomer density, and Figs. 3(b), 3(d) and 3(f) show the electrostatic potential profiles, respectively. At different charge compositions f_+, the spatial distributions of A_1 monomers in the system are similar, *i.e.*, the A_1 monomers in the system tend to accumulate closer to the center of the sphere in the B_1 phase. As the charge composition increases, the A_1 concentration becomes more widely distributed, attributed to the increased number of A_1 monomers, resulting in a looser structure. Importantly, the concentration of A_1 monomers within the central part of the core remains almost constant, independent of f_+. This indicates the saturation effect of monomer density in this region due to the complexation between oppositely charged monomers. Adding more homopolymers to the system only leads to the outspread distribution of A_1 monomers. On the other hand, with the increase in salt concentration ρ_{salt}^{add}, the distribution of A_1 monomers in the system becomes flatter, and the aggregation effect is significantly weakened due to the screening effect from the salt ions.

The electrostatic potential exhibits different trends with charge composition, as shown in Figs. 3(b), 3(d) and 3(f). At $f_+=0.3$, the negatively charged monomers are excessive, and the potential is negative overall. At $f_+=0.5$, the positively charged polymers are compensated by the negatively charged blocks. However, this situation differs from that including oppositely charged diblock copolymers, where the potential is almost zero everywhere.[43] Due to the hydrophobic effect, the charged A_1 homopolymers tend to concentrate in the central region, leading to an overall positively charged core part and a positive potential. At $f_+=0.7$, the positively charged homopolymers are excessive, and the potential is positive overall. For all charge compositions f_+, an increase in salt concentration results in a smaller magnitude of electrostatic potential, due to the shielding effect of added salts.

To gain more insight into the competition between different charged components, Figs. 4(a), 4(c) and 4(e) illustrate the distributions of $\rho_{A_1}-\rho_{A_2}$, while Figs. 4(b), 4(d) and 4(f) illustrate the net charge density ρ_e as functions of radial separation r/D for the same system as shown in Fig. 3. The profiles of $\rho_{A_1}-\rho_{A_2}$ at different f_+ display the same trend as mentioned above. However, the net charge density shows some interesting features. For each case, the net charge density at the A/B interface is almost zero. For $f_+=0.3$ or 0.5, the interface is approximately located at $r/D=0.5$, while it is $r/D=0.6$ for $f_+=0.7$. One striking characteristic is the enrichment of net charges on both sides of the interface, as shown in Figs. 4(b), 4(d) and 4(f). The enrichment indicates the preference of counterions, and its effect weakens with an increase in salt ions.

In experiments, the charge composition is an important parameter that controls the assembly properties of the system.[35,64,65] The domain size, denoted as D, as well as the

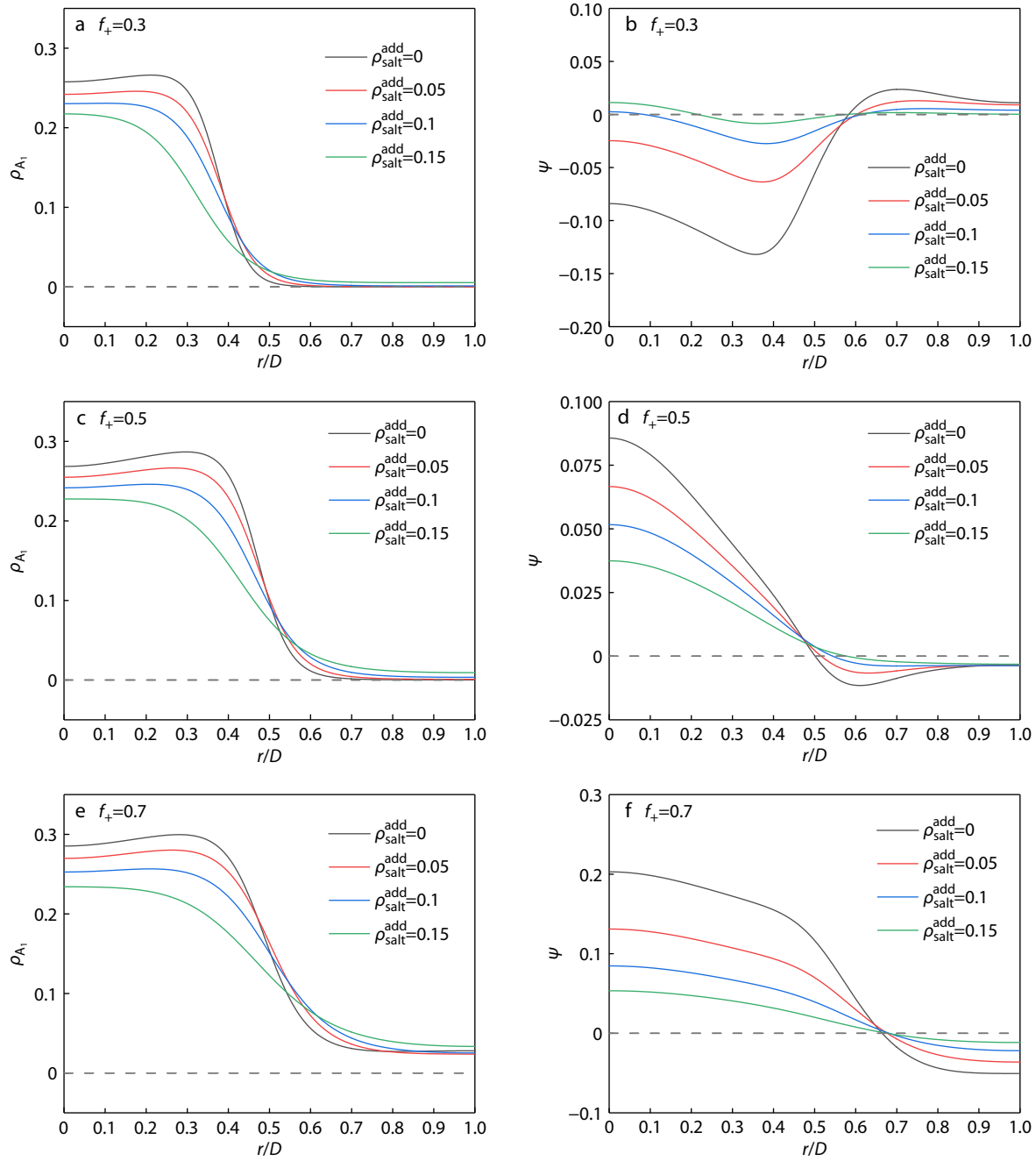

Fig. 3 Spatial distribution of concentration of A_1 monomers and electrostatic potential with different charge cases in B_1 phase at χ_{AB} = 0.05, χ_{SA} = 0.4, χ_{SB} = 0.0, N_1 = 20, N_2 = 100, f_{A_2} = 0.2, K_{ac} = 5, K_{aa} = 10, ϕ_p = 0.2. (a, b) f_+ = 0.3, (c, d) f_+ = 0.5, (e, f) f_+ = 0.7.

core size of the ordered structure, are physical quantities of general interest in experiments. Here, the core size is the typical size of the condensed phase formed by electrostatic complexation, and *D* is the domain size, as illustrated in Fig. 5. For accuracy, the boundary of the core is defined as the location with half the value between the maximum and minimum values of the A block concentrations. In the following, we only consider the B_1 phase and explore the effects of different charge compositions and salt concentrations on the domain size and core size. The results may provide useful information for regulating the self-assembled structures, even in the case of dilute solutions, where the B1 phase can be analogized to single micelles in solution.

Ordered structures can form within a certain range of the ratio, typically around f_+ = 0.05–0.9 for the salt-free system. Considering that the ratio in real experiments is often close to 0.5, we choose to focus our analysis on the range of f_+ = 0.25–0.7. Fig. 6(a) presents the domain size as a function of charge composition at different salt concentrations. Since we adopt the unit cell approximation, the domain size is equivalent to the sphere radius. Increasing the ratio of homopolymer leads to a rapid decrease in the domain size, followed by an approximate plateau around f_+ = 0.5 and then a gradual decrease. This implies that a system with a high con-

https://doi.org/10.1007/s10118-024-3080-1

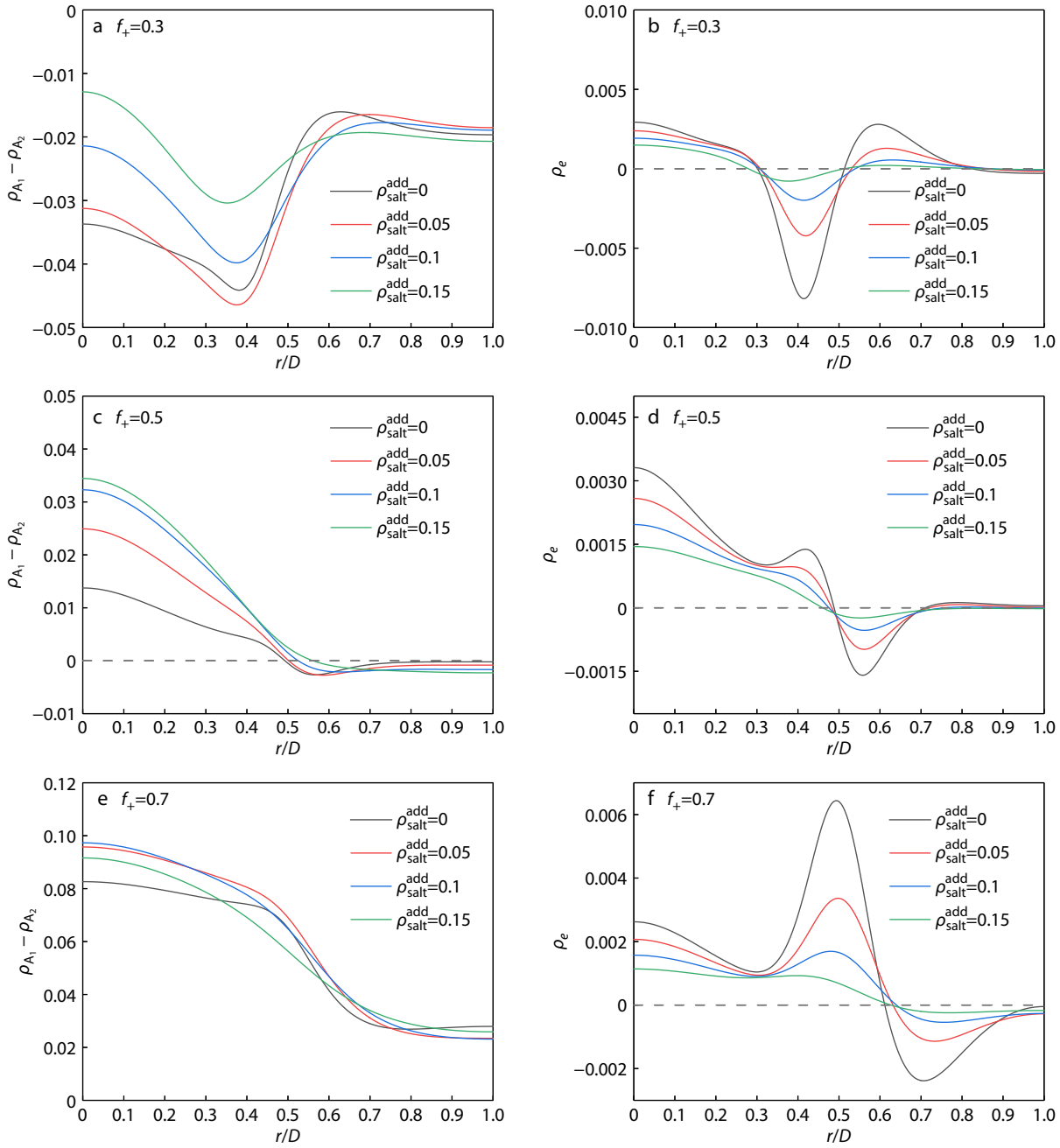

Fig. 4 Spatial distribution of concentration difference of charged monomers $\rho_{A_1} - \rho_{A_2}$ and net charge density ρ_e with different salt concentrations in B_1 phase at χ_{AB} = 0.05, χ_{SA} = 0.4, χ_{SB} = 0.0, N_1 = 20, N_2 = 100, f_{A_2} = 0.2, K_{ac} = 5, K_{aa} = 10, ϕ_p = 0.2. (a, b) f_+ = 0.3, (c, d) f_+ = 0.5, (e, f) f_+ = 0.7.

tent of positively charged homopolymers tends to self-assemble into a cubic phase with a smaller amount of diblock copolymers, resulting in a smaller size of the cubic phase. Additionally, the addition of salt ions decreases the size of the cubic phase, which may be attributed to the decreased involvement of diblock copolymers in self-assembly due to weaker electrostatic attraction from homopolymers. Furthermore, the range of the plateau region becomes smaller for larger salt concentrations. Our calculations are in good agreement with those of Lemmers' work on the triblock system[56,62] and Gohy's diblock copolymer system.[66]

In comparison, the core size of the B_1 sphere shows a different variation tendency with charge composition, as shown in Fig. 6(b). At each salt concentration, the core size is a non-monotonic function of f_+, increasing significantly and then decreasing slightly with the addition of more homopolymers. The maximum appears around f_+ = 0.5–0.6. If f_+ is smaller than 0.5, adding more homopolymers will produce stronger electrostatic repulsion between A_1 monomers, favoring an increase in core size. The subsequent slight decrease in core size at high homopolymer content probably results from enhanced electrostatic screening, as the excess polycations

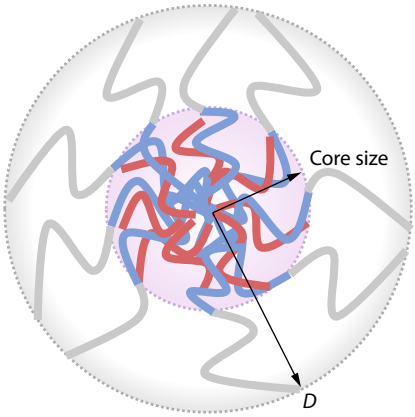

Fig. 5 Illustration of core size and D in B_1. D is the domain size of B_1 phase and core size is the radius of the complexation core.

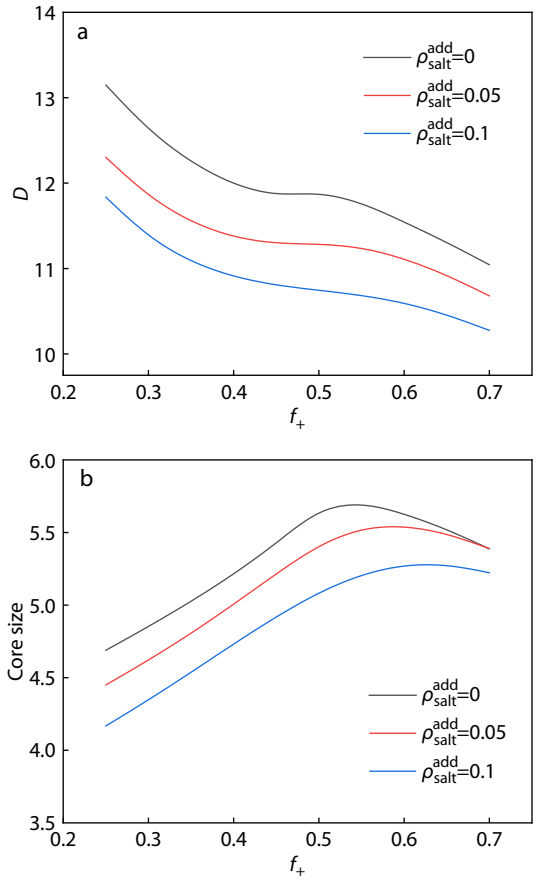

Fig. 6 Change of core size and domain size in B_1 phase with different charge cases and different salt concentrations at $\chi_{AB}=0.05$, $\chi_{SA}=0.4$, $\chi_{SB}=0.0$, $N_1=20$, $N_2=100$, $f_{A_2}=0.2$, $K_{ac}=5$, $K_{aa}=10$, $\phi_p=0.2$. (a) D, (b) core size.

have to adsorb more counterions inside the core. It is important to note that our results regarding the effect of charge composition f_+ do not match the experiments conducted by Cohen Stuart *et al.* on oppositely charged diblock-homopolymer systems in solution.[60,67] In their experiment, the pH value of the system was changed, thereby modulating the degree of ionization of polymers. The assembly behavior of the cubic phase was then regulated by charge composition in a complex way.

The Case of Hydrophilic Charged Chains

Now, we explore the system with hydrophilic charged chains. As the charged homopolymers and all blocks are hydrophilic, the

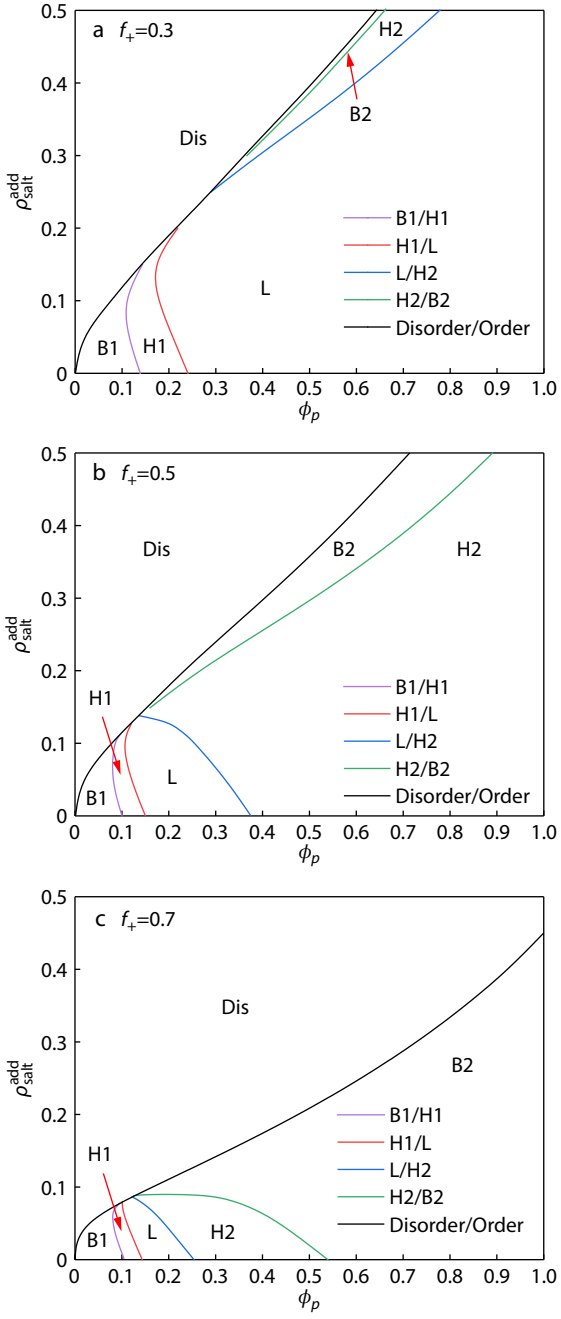

Fig. 7 Salt concentration (ρ_{salt}^{add}) versus polymer concentration (ϕ_p) phase diagram with different charge cases at $\chi_{AB}=0.05$, $\chi_{SA}=0.0$, $\chi_{SB}=0.0$, $N_1=50$, $N_2=100$, $f_{A_2}=0.5$, $K_{ac}=5$, $K_{aa}=10$. (a) $f_+=0.3$, (b) $f_+=0.5$, (c) $f_+=0.7$. Dis denotes disordered (homogeneous) phase, B_1 denotes the body-centered cubic phase with A blocks forming the cubic core, H_1 denotes the hexagonal cylinder phase with A blocks forming the cylinder core, L denotes the lamellae phase, H_2 denotes the hexagonal cylinder phase with B blocks forming the cylinder core, B_2 denotes the body-centered cubic phase with B blocks forming the cubic core.

https://doi.org/10.1007/s10118-024-3080-1

driving force of self-assembly is purely electrostatic, arising from the complexation between oppositely charged monomers. This situation is also common in real experiments.[68] To focus on the effect of charge composition, we consider a specific diblock copolymer with a charged block ratio of $f_{A_2}=0.5$. The other parameters are set as follows: $\chi_{AB}=0.05$, indicating weak incompatibility where self-assembly arises from complex coacervation. The solvent is good for both A monomers and B blocks, with $\chi_{SA}=0$ and $\chi_{SB}=0$. The chain lengths are set as $N_1=50$ and $N_2=100$.

Fig. 7 shows the salt concentration ρ_{salt}^{add} versus polymer concentration ϕ_p phase diagrams for the cases of $f_+=0.3$, 0.5, and 0.7. The ratio of homopolymers to copolymers in the system has a significant influence on the phase diagram. Several characteristics can be recognized. The first one is that the phase diagram exhibits a similar feature to the distorted phase diagram of neutral diblock copolymers. The polymer concentration plays the role of copolymer composition, while salt concentration corresponds to the temperature. The critical point occurs at certain values of ρ_{salt}^{add} and ϕ_p, at which point the phase shifts directly from the L phase to the disorder phase with increasing salt concentration. Therefore, the electrostatic screening from free ions effectively adjusts the immiscibility between A and B blocks. The second observation is that, compared with the hydrophobic system, the inverted phases B_2 and H_2 with the neutral block constituting the core phase appear. If the polycations A_1 are a minority ($f_+=0.3$), the L phase occupies the largest area in the phase diagram, and the window of the inverted B_2 phase is very narrow. If polycations can compensate polyanions completely ($f_+=0.5$), then the L phase becomes much smaller, and the H_2 phase dominates the phase diagram. Increasing the charge composition further ($f_+=0.7$) leads to the B_2 phase having the largest area.

CONCLUSIONS

We extended the SCFT method to investigate the self-assembly of a mixture of block polyelectrolytes driven by electrostatic complexation between oppositely charged chains, particularly focusing on systems consisting of diblock copolymers and homopolymers with opposite charges. This method primarily relies on the association of "ion-pairs," encompassing ion-pairs formed by polycation/polyanion binding or by polyelectrolyte/counterion binding. We systematically calculated phase diagrams in salt concentration versus polymer concentration space, providing insights into the corresponding monomer concentration distributions and electrostatic potential distributions under various parameter conditions.

Our focus was on understanding the influence of charge composition on the microstructure, particularly in cases where the hydrophobic charged A blocks are in the minority. The core part of the ordered phase is constituted by the complexed segment from charged polymers. Increasing the charge ratio from the positively charged homopolymer induces a phase transition from B_1 to H_1 to L phase. Additionally, the domain spacing is a decreasing function of charge composition, while the core size of the complexation part increases initially and then decreases slightly with an increase in charge composition. If the charged blocks are hydrophilic and their lengths equal that of the neutral blocks, inverse phases with the core formed by neutral blocks may appear in the phase diagram. The window of inverse phases may considerably increase with an increase in charge composition.

The variation in charge composition represents a unique feature of two-component polyelectrolyte systems. We studied the influence of this factor on the formation of ordered phases for the first time. Adjusting the charge composition to off-stoichiometric conditions easily creates opportunities for further tuning the morphologies and physical properties of self-assembled microstructures.

Conflict of Interests

The authors declare no interest conflict.

ACKNOWLEDGMENTS

This work was financially supported by the National Natural Science Foundation of China (NSFC) (Nos. 22073002, 51921002 and 22373008).

REFERENCES

1 Zhou, J.; Shi, A. C. Microphase separation induced by differential interactions in diblock copolymer/homopolymer blends. *J. Chem. Phys.* **2009**, 130, 234904.
2 Qian, H. J.; Lu, Z. Y.; Chen, L. J.; Li, Z. S.; Sun, C. C. Dissipative particle dynamics study on the interfaces in incompatible A/B homopolymer blends and with their block copolymers. *J. Chem. Phys.* **2005**, 122, 184907.
3 Hashimoto, T.; Koizumi, S.; Hasegawa, H.; Izumitani, T.; Hyde, S. T. Observation of "mesh" and "strut" structures in block copolymer/homopolymer mixtures. *Macromolecules* **1992**, 25, 1433–1439.
4 Han, C. D.; Baek, D. M.; Kim, J.; Kimishima, K.; Hashimoto, T. Viscoelastic behavior, phase equilibria, and microdomain morphology in mixtures of a block copolymer and a homopolymer. *Macromolecules* **1992**, 25, 3052–3067.
5 Spontak, R. J.; Smith, S. D.; Ashraf, A. Dependence of the OBDD morphology on diblock copolymer molecular weight in copolymer/homopolymer blends. *Macromolecules* **1993**, 26, 956–962.
6 Disko, M. M.; Liang, K. S.; Behal, S. K.; Roe, R. J.; Jeon, K. J. Catenoid-lamellar phase in blends of styrene-butadiene diblock copolymer and homopolymer. *Macromolecules* **1993**, 26, 2983–2986.
7 Jeon, K. J.; Roe, R. J. Solubilization of a homopolymer in a block copolymer. *Macromolecules* **1994**, 27, 2439–2447.
8 Zin, W. C.; Roe, R. J. Phase equilibria and transition in mixtures of a homopolymer and a block copolymer. 1. Small-angle X-ray scattering study. *Macromolecules* **1984**, 17, 183–188.
9 Roe, R. J.; Zin, W. C. Phase equilibria and transition in mixtures of a homopolymer and a block copolymer. 2. Phase diagram. *Macromolecules* **1984**, 17, 189–194.
10 Kinning, D. J.; Winey, K. I.; Thomas, E. L. Structural transitions from spherical to nonspherical micelles in blends of poly(styrene-butadiene) diblock copolymer and polystyrene homopolymers. *Macromolecules* **1988**, 21, 3502–3506.
11 Owens, J. N.; Gancarz, I. S.; Koberstein, J. T.; Russell, T. P. Order-disorder transitions in mixtures of homopolymers with diblock

copolymers. *Macromolecules* **1989**, 22, 3388–3394.
12 Hashimoto, T.; Tanaka, H.; Hasegawa, H. Ordered structure in mixtures of a block copolymer and homopolymers. 2. Effects of molecular weights of homopolymers. *Macromolecules* **1990**, 23, 4378–4386.
13 Kuo, S. W. Hydrogen bonding mediated self-assembled structures from block copolymer mixtures to mesoporous materials. *Polymer International* **2022**, 71, 393–410.
14 Matsen, M. W. Phase behavior of block copolymer/homopolymer blends. *Macromolecules* **1995**, 28, 5765–5773.
15 Matsen, M. W. Stabilizing new morphologies by blending homopolymer with block copolymer. *Physical Review Letters* **1995**, 74, 4225–4228.
16 Matsen, M. W. New fast SCFT algorithm applied to binary diblock copolymer/homopolymer blends. *Macromolecules* **2003**, 36, 9647–9657.
17 Lee, H. F.; Kuo, S. W.; Huang, C. F.; Lu, J. S.; Chan, S. C.; Wang, C. F.; Chang, F. C. Hydrogen-bonding interactions mediate the phase behavior of an A-B/C block copolymer/homopolymer blend comprising poly(methyl methacrylate-*b*-vinylpyrrolidone) and Poly(Vinylphenol). *Macromolecules* **2006**, 39, 5458–5465.
18 Chen, W. C.; Kuo, S. W.; Lu, C. H.; Jeng, U. S.; Chang, F. C. Self-assembly structures through competitive interactions of crystalline-amorphous diblock copolymer/homopolymer blends: poly(ε-caprolactone-*b*-4-vinyl pyridine)/poly(vinyl phenol). *Macromolecules* **2009**, 42, 3580–3590.
19 Dobrosielska, K.; Wakao, S.; Suzuki, J.; Noda, K.; Takano, A.; Matsushita, Y. Effect of homopolymer molecular weight on nanophase-separated structures of AB block copolymer/C homopolymer blends with hydrogen-bonding interactions. *Macromolecules* **2009**, 42, 7098–7102.
20 Dehghan, A.; Shi, A. C. Modeling hydrogen bonding in diblock copolymer/homopolymer blends. *Macromolecules* **2013**, 46, 5796–5805.
21 Voets, I. K.; de Keizer, A.; de Waard, P.; Frederik, P. M.; Bomans, P. H. H.; Schmalz, H.; Walther, A.; King, S. M.; Leermakers, F. A. M.; Cohen Stuart, M. A. Double-faced micelles from water-soluble polymers. *Angew. Chem., Int. Ed.* **2006**, 45, 6673–6676.
22 Takahashi, R.; Sato, T.; Terao, K.; Yusa, S. I. Intermolecular interactions and self-assembly in aqueous solution of a mixture of anionic-neutral and cationic-neutral block copolymers. *Macromolecules* **2015**, 48, 7222–7229.
23 Yan, Y.; Harnau, L.; Besseling, N. A. M.; de Keizer, A.; Ballauff, M.; Rosenfeldt, S.; Cohen Stuart, M. A. Spherocylindrical coacervate core micelles formed by a supramolecular coordination polymer and a diblock copolymer. *Soft Matter* **2008**, 4, 2207–2212.
24 Oana, H.; Morinaga, M.; Kishimura, A.; Kataoka, K.; Washizu, M. Direct formation of giant unilamellar vesicles from microparticles of polyion complexes and investigation of their properties using a microfluidic chamber. *Soft Matter* **2013**, 9, 5448–5458.
25 Anraku, Y.; Kishimura, A.; Oba, M.; Yamasaki, Y.; Kataoka, K. Spontaneous formation of nanosized unilamellar polyion complex vesicles with tunable size and properties. *J. Am. Chem. Soc.* **2010**, 132, 1631–1636.
26 Perry, S. L.; Leon, L.; Hoffmann, K. Q.; Kade, M. J.; Priftis, D.; Black, K. A.; Wong, D.; Klein, R. A.; Pierce, C. F.; Margossian, K. O.; Whitmer, J. K.; Qin, J.; de Pablo, J. J.; Tirrell, M. Chirality-selected phase behaviour in ionic polypeptide complexes. *Nat. Commun.* **2015**, 6, 6052.
27 Elabd, Y. A.; Hickner, M. A. Block copolymers for fuel cells. *Macromolecules* **2011**, 44, 1–11.
28 Rubatat, L.; Shi, Z.; Diat, O.; Holdcroft, S.; Frisken, B. J. Structural study of proton-conducting fluorous block copolymer membranes. *Macromolecules* **2006**, 39, 720–730.
29 Wang, X.; Yakovlev, S.; Beers, K. M.; Park, M. J.; Mullin, S. A.; Downing, K. H.; Balsara, N. P. On the origin of slow changes in ionic conductivity of model block copolymer electrolyte membranes in contact with humid air. *Macromolecules* **2010**, 43, 5306–5314.
30 LimSoo, P.; Luo, L.; Maysinger, D.; Eisenberg, A. Incorporation and release of hydrophobic probes in biocompatible polycaprolactone-block-poly(ethylene oxide) micelles: implications for drug delivery. *Langmuir* **2002**, 18, 9996–10004.
31 Acar, H.; Ting, J. M.; Srivastava, S.; LaBelle, J. L.; Tirrell, M. V. Molecular engineering solutions for therapeutic peptide delivery. *Chem. Soc. Rev* **2017**, 46, 6553–6569.
32 Chassenieux, C.; Tsitsilianis, C. Recent trends in pH/thermo-responsive self-assembling hydrogels: from polyions to peptide-based polymeric gelators. *Soft Matter* **2016**, 12, 1344–1359.
33 Huo, H.; Zhao, W.; Duan, X.; Sun, Z. Y. Control of diblock copolyelectrolyte morphology through electric field application. *Macromolecules* **2023**, 56, 1065–1076.
34 Rahalkar, A.; Wei, G.; Nieuwendaal, R.; Prabhu, V. M.; Srivastava, S.; Levi, A. E.; Pablo, J. J. d.; Tirrell, M. V. Effect of temperature on the structure and dynamics of triblock polyelectrolyte gels. *J. Chem. Phys.* **2018**, 149, 163310.
35 Lemmers, M.; Sprakel, J.; Voets, I. K.; van der Gucht, J.; Cohen Stuart, M. A. Multiresponsive reversible gels based on charge-driven assembly. *Angew. Chem., Int. Ed.* **2010**, 49, 708–711.
36 Kramarenko, E. Y.; Khokhlov, A. R.; Reineker, P. Stoichiometric polyelectrolyte complexes of ionic block copolymers and oppositely charged polyions. *J. Chem. Phys.* **2006**, 125, 194902.
37 Duan, X.; Shi, A. C.; An, L. Formation of ionomer microparticles via polyelectrolyte complexation. *Macromolecules* **2021**, 54, 9053–9062.
38 Hunt, J. N.; Feldman, K. E.; Lynd, N. A.; Deek, J.; Campos, L. M.; Spruell, J. M.; Hernandez, B. M.; Kramer, E. J.; Hawker, C. J. Tunable, high modulus hydrogels driven by ionic coacervation. *Adv. Mater.* **2011**, 23, 2327–2331.
39 Krogstad, D. V.; Lynd, N. A.; Choi, S. H.; Spruell, J. M.; Hawker, C. J.; Kramer, E. J.; Tirrell, M. V. Effects of polymer and salt concentration on the structure and properties of triblock copolymer coacervate hydrogels. *Macromolecules* **2013**, 46, 1512–1518.
40 Audus, D. J.; Gopez, J. D.; Krogstad, D. V.; Lynd, N. A.; Kramer, E. J.; Hawker, C. J.; Fredrickson, G. H. Phase behavior of electrostatically complexed polyelectrolyte gels using an embedded fluctuation model. *Soft Matter* **2015**, 11, 1214–1225.
41 Lytle, T. K.; Radhakrishna, M.; Sing, C. E. High charge density coacervate assembly *via* hybrid monte carlo single chain in mean field theory. *Macromolecules* **2016**, 49, 9693–9705.
42 Jiang, J.; Chen, X.; Yang, S.; Chen, E. Q. The size and affinity effect of counterions on self-assembly of charged block copolymers. *J. Chem. Phys.* **2020**, 152, 124901.
43 Jiang, J.; Chen, E. Q.; Yang, S. The effect of ion pairs on coacervate-driven self-assembly of block polyelectrolytes. *J. Chem. Phys.* **2021**, 154, 144903.
44 Holappa, S.; Andersson, T.; Kantonen, L.; Plattner, P.; Tenhu, H. Soluble polyelectrolyte complexes composed of poly(ethylene oxide)-block-poly(sodium methacrylate) and poly(methacryloyloxyethyl trimethylammonium chloride). *Polymer* **2003**, 44, 7907–7916.
45 Marras, A. E.; Vieregg, J. R.; Ting, J. M.; Rubien, J. D.; Tirrell, M. V. Polyelectrolyte complexation of oligonucleotides by charged hydrophobic-neutral hydrophilic block copolymers. *Polymers* **2019**, 11, 83.
46 ElJundi, A.; Buwalda, S. J.; Bakkour, Y.; Garric, X.; Nottelet, B. Double hydrophilic block copolymers self-assemblies in biomedical applications. *Adv. Colloid Interface Sci.* **2020**, 283, 102213.

https://doi.org/10.1007/s10118-024-3080-1

47 Hofs, B.; de Keizer, A.; van der Burgh, S.; Leermakers, F. A. M.; Cohen Stuart, M. A.; Millard, P. E.; Müller, A. H. E. Complex coacervate core micro-emulsions. *Soft Matter* **2008**, 4, 1473–1482.

48 Lindhoud, S.; de Vries, R.; Schweins, R.; Cohen Stuart, M. A.; Norde, W. Salt-induced release of lipase from polyelectrolyte complex micelles. *Soft Matter* **2009**, 5, 242–250.

49 Read, E.; Lonetti, B.; Gineste, S.; Sutton, A. T.; Di Cola, E.; Castignolles, P.; Gaborieau, M.; Mingotaud, A. F.; Destarac, M.; Marty, J. D. Mechanistic insights into the formation of polyion complex aggregates from cationic thermoresponsive diblock copolymers. *J. Colloid Interface Sci.* **2021**, 590, 268–276.

50 Rizis, G.; van de Ven, T. G. M.; Eisenberg, A. Homopolymers as structure-driving agents in semicrystalline block copolymer micelles. *ACS Nano* **2015**, 9, 3627–3640.

51 van der Burgh, S.; de Keizer, A.; Cohen Stuart, M. A. Complex coacervation core micelles. Colloidal stability and aggregation mechanism. *Langmuir* **2004**, 20, 1073–1084.

52 Weaver, J. V. M.; Armes, S. P.; Liu, S. A "holy trinit" of micellar aggregates in aqueous solution at ambient temperature: unprecedented self-assembly behavior from a binary mixture of a neutral-cationic diblock copolymer and an anionic polyelectrolyte. *Macromolecules* **2003**, 36, 9994–9998.

53 Liu, J. Y.; Song, H. R.; Wang, M.; Jin, S. H.; Liang, Z.; Mao, X.; Li, W.; Deng, R. H.; Zhu, J. T. Asymmetric mesoporous carbon microparticles by 3D-confined self-assembly of block copolymer/homopolymer blends and selective carbonization. *Chinese J. Polym. Sci.* **2023**, 41, 787–793.

54 Zhang, X.; Chen, J.; Xu, L.; Liu, T. Supramolecular self-assembly behaviors of asymmetric diblock copolymer blends with hydrogen bonding interactions between shorter blocks modelled by Yukawa potentials. *Chinese J. Polym. Sci.* **2021**, 39, 1502–1509.

55 Kramarenko, E. Y.; Khokhlov, A. R.; Reineker, P. Micelle formation in a dilute solution of block copolymers with a polyelectrolyte block complexed with oppositely charged linear chains. *J. Chem. Phys.* **2003**, 119, 4945–4952.

56 Lemmers, M.; Voets, I. K.; Cohen Stuart, M. A.; der Gucht, J. V. Transient network topology of interconnected polyelectrolyte complex micelles. *Soft Matter* **2011**, 7, 1378–1389.

57 Bodrova, A. S.; Kramarenko, E. Y.; Potemkin, I. I. Microphase separation induced by complexation of ionic-non-ionic diblock copolymers with oppositely charged linear chains. *Macromolecules* **2010**, 43, 2622–2629.

58 Harada, A.; Kataoka, K. Formation of polyion complex micelles in an aqueous milieu from a pair of oppositely-charged block copolymers with poly(ethylene glycol) segments. *Macromolecules* **1995**, 28, 5294–5299.

59 CohenStuart, M. A.; Besseling, N. A. M.; Fokkink, R. G. Formation of micelles with complex coacervate cores. *Langmuir* **1998**, 14, 6846–6849.

60 Voets, I. K.; de Keizer, A.; Cohen Stuart, M. A.; Justynska, J.; Schlaad, H. Irreversible structural transitions in mixed micelles of oppositely charged diblock copolymers in aqueous solution. *Macromolecules* **2007**, 40, 2158–2164.

61 Lindhoud, S.; Norde, W.; Cohen Stuart, M. A. Reversibility and relaxation behavior of polyelectrolyte complex micelle formation. *J. Phys. Chem. B* **2009**, 113, 5431–5439.

62 Lemmers, M.; Spruijt, E.; Beun, L.; Fokkink, R.; Leermakers, F.; Portale, G.; Cohen Stuart, M. A.; van der Gucht, J. The influence of charge ratio on transient networks of polyelectrolyte complex micelles. *Soft Matter* **2012**, 8, 104–117.

63 Shi, A. C.; Noolandi, J. Theory of inhomogeneous weakly charged polyelectrolytes. *Macromol. Theory Simul.* **1999**, 8, 214–229.

64 Yan, Y.; Besseling, N. A. M.; de Keizer, A.; Marcelis, A. T. M.; Drechsler, M.; Cohen Stuart, M. A. Hierarchical self-assembly in solutions containing metal ions, ligand, and diblock copolymer. *Angew. Chem., Int. Ed.* **2007**, 46, 1807–1809.

65 Nakai, K.; Nishiuchi, M.; Inoue, M.; Ishihara, K.; Sanada, Y.; Sakurai, K.; Yusa, S. I. Preparation and characterization of polyion complex micelles with phosphobetaine shells. *Langmuir* **2013**, 29, 9651–9661.

66 Gohy, J. F.; Varshney, S. K.; Antoun, S.; Jérôme, R. Water-soluble complexes formed by sodium poly(4-styrenesulfonate) and a poly(2-vinylpyridinium)-block-poly(ethyleneoxide) copolymer. *Macromolecules* **2000**, 33, 9298–9305.

67 Hofs, B.; de Keizer, A.; Cohen Stuart, M. A. On the stability of (highly aggregated) polyelectrolyte complexes containing a charged-block-neutral diblock copolymer. *J. Phys. Chem. B* **2007**, 111, 5621–5627.

68 Yusa, S. I.; Fukuda, K.; Yamamoto, T.; Ishihara, K.; Morishima, Y. Synthesis of well-defined amphiphilic block copolymers having phospholipid polymer sequences as a novel biocompatible polymer micelle reagent. *Biomacromolecules* **2005**, 6, 663–670.

https://doi.org/10.1007/s10118-024-3080-1